

Precise Temperature Compensation of Phase in a Rhythmic Motor Pattern

Lamont S. Tang, Marie L. Goeritz, Jonathan S. Caplan, Adam L. Taylor, Mehmet Fisek, Eve Marder*

Volen Center and Biology Department, Brandeis University, Waltham, Massachusetts, United States of America

Abstract

Most animal species are cold-blooded, and their neuronal circuits must maintain function despite environmental temperature fluctuations. The central pattern generating circuits that produce rhythmic motor patterns depend on the orderly activation of circuit neurons. We describe the effects of temperature on the pyloric rhythm of the stomatogastric ganglion of the crab, *Cancer borealis*. The pyloric rhythm is a triphasic motor pattern in which the Pyloric Dilator (PD), Lateral Pyloric (LP), and Pyloric (PY) neurons fire in a repeating sequence. While the frequency of the pyloric rhythm increased about 4-fold ($Q_{10} \sim 2.3$) as the temperature was shifted from 7°C to 23°C, the phase relationships of the PD, LP, and PY neurons showed almost perfect temperature compensation. The Q_{10} 's of the input conductance, synaptic currents, transient outward current (I_A), and the hyperpolarization-activated inward current (I_H), all of which help determine the phase of LP neuron activity, ranged from 1.8 to 4. We studied the effects of temperature in >1,000 computational models (with different sets of maximal conductances) of a bursting neuron and the LP neuron. Many bursting models failed to monotonically increase in frequency as temperature increased. Temperature compensation of LP neuron phase was facilitated when model neurons' currents had Q_{10} 's close to 2. Together, these data indicate that although diverse sets of maximal conductances may be found in identified neurons across animals, there may be strong evolutionary pressure to restrict the Q_{10} 's of the processes that contribute to temperature compensation of neuronal circuits.

Citation: Tang LS, Goeritz ML, Caplan JS, Taylor AL, Fisek M, et al. (2010) Precise Temperature Compensation of Phase in a Rhythmic Motor Pattern. PLoS Biol 8(8): e1000469. doi:10.1371/journal.pbio.1000469

Academic Editor: William A. Harris, University of Cambridge, United Kingdom

Received: February 1, 2010; **Accepted:** July 20, 2010; **Published:** August 31, 2010

Copyright: © 2010 Tang et al. This is an open-access article distributed under the terms of the Creative Commons Attribution License, which permits unrestricted use, distribution, and reproduction in any medium, provided the original author and source are credited.

Funding: This work was funded by the National Institute of Health grants 2P01 NS-044232, MH 46742, and IGERT DGE 0549390. The funders had no role in study design, data collection and analysis, decision to publish, or preparation of the manuscript.

Competing Interests: The authors have declared that no competing interests exist.

Abbreviations: AB, Anterior Burster; IPSCs, Inhibitory Postsynaptic Currents; IPSPs, Inhibitory Postsynaptic Potentials; PD, Pyloric Dilator; PTX, picrotoxin; PY, Pyloric; STG, stomatogastric ganglion; TTX, tetrodotoxin

* E-mail: marder@brandeis.edu

Introduction

The nervous systems of cold-blooded animals must function across significant ranges of temperature despite the fact that the signal transduction pathways and synaptic and intrinsic membrane currents are all temperature-dependent. This is particularly intriguing because one would not expect all cellular processes to have the same temperature dependence, and therefore it is hard to imagine that functional circuit integrity would necessarily be easily maintained when temperature is altered. Nonetheless, temperature compensation, that is maintenance of constant function as temperature is altered, is an important property of circadian rhythms [1,2] and has been reported in other systems as well [3].

All biological processes have characteristic Q_{10} 's that describe the changes in their rates as a function of temperature. Although the Q_{10} for many biological processes is ~ 2 , Q_{10} 's for ion channels can vary from 1.5 to almost 100. For example, the Q_{10} 's for activation and inactivation of some K^+ channels are 1.8–4.6 [4], many temperature sensing TRP channels have Q_{10} 's higher than 10 [5], and some Ca^{2+} channels have inactivation rates with Q_{10} 's as high as 19 [6]. How different can the various Q_{10} 's that govern the intrinsic and synaptic conductances within a circuit be and still allow appropriate function to be maintained despite environmental temperature change? Which attributes of circuit performance

are temperature dependent and which, if any, are temperature compensated?

Cancer borealis, the crab used for this study, lives in the northern Atlantic Ocean, and can be found from Newfoundland to Florida [7,8,9]. While most *C. borealis* inhabit deeper waters (at depths of 800 m), they also are frequently found in both intertidal and subtidal ecosystems foraging for food [7,8,9,10,11]. During the summer at these shallow depths (ranging from 0–10 m), *C. borealis* can experience temperature fluctuations ranging from 8°C to 24°C within a single day [10,11]. During the winter, *C. borealis* is found at ocean temperatures ranging from 3°C to 16°C [8]. Presumably, the nervous system of these animals can cope with such considerable temperature fluctuations.

The stomatogastric ganglion (STG) of marine crustaceans generates two motor patterns that are responsible for the chewing and filtering of food [12]. The pyloric rhythm is a triphasic motor pattern driven by a three-neuron pacemaker ensemble (the single Anterior Burster (AB) and two Pyloric Dilator (PD) neurons). The Lateral Pyloric (LP) and Pyloric (PY) neurons fire on rebound from inhibition by the pacemaker neurons. Previous work has indicated that a number of processes can influence the phase of the LP and PY neurons' rebound firing. These include the strength and time course of the inhibitory synapses that the LP and PY neurons receive from the AB and PD neurons [13,14,15] and the

Author Summary

The neural circuits that produce behaviors such as walking, chewing, and swimming must be both robust and flexible to changing internal and environmental demands. How then do cold-blooded animals cope with temperature fluctuations when the underlying processes that give rise to circuit performance are themselves temperature-dependent? We exploit the crab stomatogastric ganglion to understand the extent to which circuit features are robust to temperature perturbations. We subjected these circuits to temperature ranges they normally encounter in the wild. Interestingly, while the frequency of activity in the network increased 4-fold over these temperature ranges, the relative timing between neurons in the network—termed phase relationships—remained constant. To understand how temperature compensation of phase might occur, we characterized the temperature dependence (Q_{10} 's) of synapses and membrane currents. We used computational models to show that the experimentally measured Q_{10} 's can promote phase maintenance. We also showed that many model bursting neurons fail to burst over the entire temperature range and that phase maintenance is promoted by closely restricting the model neurons' Q_{10} 's. These results imply that although ion channel numbers can vary between individuals, there may be strong evolutionary pressure that restricts the temperature dependence of the processes that contribute to temperature compensation of neuronal circuits.

conductances of the transient outward K^+ current (I_A) and the hyperpolarization-activated inward current (I_h) [16,17,18].

The phase relationships of the network neurons are maintained relatively constant as a function of frequency [15,19,20,21,22,23] and during the animal's growth [19,24]. This phase constancy over a range of frequencies has been extensively studied in preparations held at constant temperature. We now show that although temperature drastically alters the frequency of the pyloric rhythm, its phase relationships are remarkably temperature invariant. This motivated us to examine the effects of temperature on the synaptic and intrinsic membrane currents that have been previously implicated in the control of phase in the pyloric rhythm. By so doing, we attempt to account for the temperature compensation of pyloric rhythm phase in terms of the effects of temperature on some of its membrane conductances.

Although the pyloric rhythm is a “simple” neuronal circuit, its dynamics involve the activation and inactivation of many intrinsic and synaptic currents. To determine whether the biological results “automatically” arise from the effects of temperature on membrane currents with similar Q_{10} 's, we varied temperature in two different computational models, one of a bursting pacemaker neuron [25] and one of the LP neuron [26].

Results

Effects of Temperature on the Pyloric Rhythm

The triphasic pyloric rhythm of the STG is shown in the extracellular recordings from the motor nerves exiting the STG in Figure 1A. The top trace shows a burst of the PD neurons, the second trace shows the activity of the LP neuron, and the bottom trace shows the activity of the PY neurons. By convention, we call

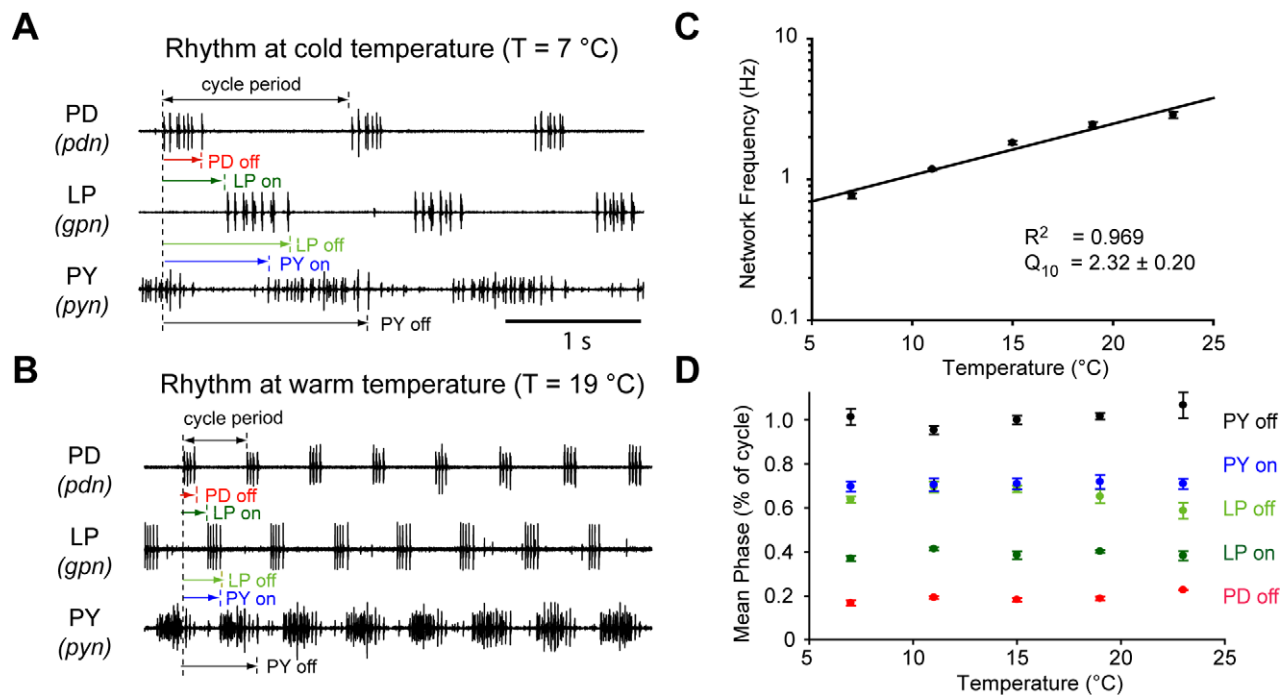


Figure 1. Quantification of pyloric network output at different temperatures. (A) Example extracellular nerve recordings of the pyloric rhythm at cold temperature ($T = 7^\circ\text{C}$). The onset and offset delay of each neuron relative to the onset of PD neuron burst are indicated. Horizontal scale bar, 1 s, for both (A) and (B). (B) Example extracellular nerve recordings from the same preparation as in (A) but at warm temperature ($T = 19^\circ\text{C}$). The same delay measurements are indicated as in (A). (C) The frequency of the pyloric rhythm plotted as a function of temperature from $T = 7^\circ\text{C}$ to $T = 23^\circ\text{C}$ ($n = 7$). (D) The mean phase (delay divided by cycle period) values of the pyloric rhythm plotted as a function of temperature from $T = 7^\circ\text{C}$ to $T = 23^\circ\text{C}$ ($n = 7$).

doi:10.1371/journal.pbio.1000469.g001

the beginning of the PD neuron burst the start of the pyloric rhythm cycle, and the other neurons are referenced to the PD neuron activity. One cycle period is defined as the time between the start of one PD burst and that of the subsequent PD burst. The phases at which each neuron burst starts and ends are defined as the delays to those events divided by the cycle period.

All of the animals used in this study were acclimated to 11°C for at least 3 wk before use. The frequency of the pyloric rhythms from 23 animals at 11°C varied from 1.0 Hz to 1.5 Hz and exhibited a mean frequency of 1.20 ± 0.11 Hz (S.D.). The median pyloric frequency of these acclimated animals was not significantly different from that of a non-acclimated population described previously ($p = 0.35$, Mann-Whitney rank sum test, $n = 45$ for the non-acclimated population) [15]. Interestingly, the variance of pyloric frequency in the acclimated population was lower than that in the non-acclimated population (S.D. = 0.21, $p < 0.05$, Levene test).

To quantify the effects of temperature on frequency and phase of the pyloric rhythm, we recorded from the motor nerves in seven preparations that were gradually warmed from 7°C to 23°C (Figure 1). Figure 1A shows the pyloric rhythm at 7°C, and Figure 1B shows recordings from the same preparation at 19°C. Note that the frequency increased substantially, but the relative timing of the triphasic pattern of activity was largely preserved. Figure 1C presents the data pooled from the seven experiments. Over this temperature range the frequency increased about 4-fold from 0.7 ± 0.1 Hz to 2.9 ± 0.4 Hz (S.D.), with a Q_{10} of 2.32 ± 0.2 (Table 1). Temperature had a significant effect on pyloric frequency ($p < 0.01$, one-way repeated measures ANOVA, $n = 7$). Remarkably, although the frequency varied considerably as a function of temperature, the phase of firing of the pyloric neurons was virtually unaltered by temperature (Figure 1D, $n = 7$), as indicated by Q_{10} 's not significantly different from 1 (Table 1). We did not find evidence for hysteresis as there was no statistically significant difference between increasing temperature from 7 to

23°C versus decreasing temperature from 23 to 7°C ($p = 0.410$, two-way repeated ANOVA, $n = 4$).

The Effects of Temperature on Membrane Potential Trajectories

To gain further insight into how phase relationships might remain stable despite the increase in frequency as a function of temperature, we examined the intracellular waveforms of the pyloric neurons as a function of temperature. Figure 2A shows simultaneous intracellular recordings from the PD, LP, and PY neurons in a single preparation at temperatures from 7°C to 23°C (circuit diagram; Figure 2B). Again, while the frequency dramatically increased, the characteristic triphasic motor pattern was maintained, and the intracellular waveforms were similar at all temperatures. This can be seen most effectively by scaling the membrane potential trajectories of the intracellular waveforms to the cycle period (Figure 2C). The membrane potential trajectories of the pyloric neurons are very similar when they are temporally scaled.

Figure 2B shows a simplified connectivity diagram for the pyloric rhythm, and illustrates that the LP neuron is inhibited by the pacemaker neurons and the PY neurons. The phase of LP firing is known to depend both on its synaptic inputs (Figure 2B) and on its intrinsic, voltage-dependent membrane currents [13,14,17,18,27,28,29]. The effects of temperature on the Inhibitory Postsynaptic Potentials (IPSPs) recorded in the LP neuron are plotted in Figure 2D. Note that this is a measure of the combined, total IPSP, consisting of the IPSP evoked first by the PY neurons, followed by the IPSPs evoked by the AB and PD neurons (Figure 2C). We measured the total IPSP as the amplitude of the membrane potential excursion from the end of the LP burst to its most hyperpolarized value (the first component comes from the PY neurons, and the second sharp hyperpolarization from PD/AB neuron activity). The total IPSPs recorded in LP were not statistically different over the temperature range shown ($Q_{10} = 0.92 \pm 0.1$, $p = 0.256$, one-way repeated measures ANOVA; Table 1).

Effects of Temperature on Synaptic Currents

Although the total IPSPs in LP are temperature compensated, this does not necessarily mean that the synaptic currents are also constant, as the IPSP waveform and amplitude depend on the other membrane conductances and time constants as well as the synaptic current. We measured the LP neuron input conductance in voltage clamp as a function of temperature by applying tetrodotoxin (TTX) and picrotoxin (PTX) to remove action potentials and block most of the synaptic inputs to the LP neuron. We then stepped the voltage from -60 mV to -80 mV in 5 mV steps, measured the resulting currents, and calculated the input conductance. Figure 3A shows that the input conductance increased with temperature ($p < 0.002$, one-way repeated measures ANOVA), with a Q_{10} of 1.56 ± 0.17 .

The apparent lack of change in IPSP amplitude from 7°C to 23°C despite a nearly 2-fold increase in input conductance over that range was intriguing. Therefore, we voltage-clamped the LP neuron during the ongoing pyloric rhythm and directly measured the total Inhibitory Postsynaptic Currents (IPSCs) over the same range of temperatures. Figures 3B and 3C show the IPSCs measured at 7°C and 19°C at three different voltages, -60 mV, -80 mV, and -100 mV. The timing of PY and PD neuron activity is shown below the IPSC recordings so that the PY and AB/PD components of the IPSCs can be seen. At -60 mV at 7°C there was little or no net current seen during PY time, but the current was clearly outward during PD time. At 19°C a small

Table 1. Temperature dependence of pyloric network parameters.

Level	Process	Q_{10}	S.E.	$m \neq 0?$	p Value
Network	Cycle Frequency	2.32	0.20	yes	<0.001
Phase Relationships	PD off	1.02*	0.07	no	0.083
	LP on	1.00*	0.04	no	0.887
	LP off	0.94*	0.05	no	0.322
	PY on	1.01*	0.01	no	0.090
	PY off	1.04*	0.03	no	0.223
Synaptic	IPSPs onto LP neuron	0.92*	0.10	no	0.256
	IPSCs onto LP neuron	2.29	0.25	yes	<0.001
LP Membrane	g_A	1.90	0.44	yes	<0.001
Currents	I_A activation rate	3.00	0.16	yes	<0.001
	I_A inactivation rate	3.78	0.18	yes	<0.001
	g_h	3.13	0.46	yes	<0.001
	I_h activation rate	3.36	0.18	yes	<0.001
Input Conductance		1.56	0.17	yes	<0.001

*These Q_{10} 's were highlighted for their low temperature sensitivities (i.e., $Q_{10} \sim 1$). To test whether the slopes (m) of these Q_{10} 's were significantly different than zero, t tests and their associated p values are reported in the right-hand columns.

doi:10.1371/journal.pbio.1000469.t001

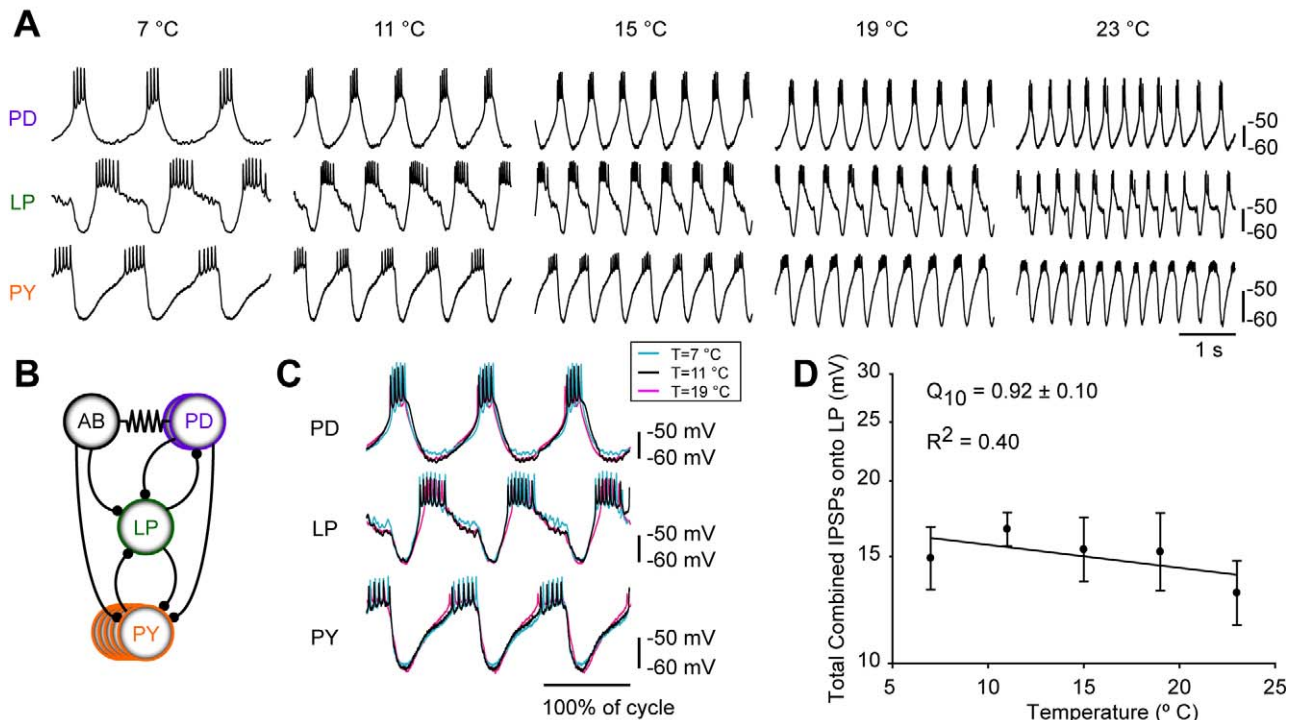


Figure 2. Similarity of membrane potential trajectories and IPSPs of the pyloric neurons at different temperatures. (A) Simultaneous intracellular recordings of PD, LP, and PY neurons of the pyloric rhythm at different temperatures ($T = 7, 11, 15, 19,$ and 23°C , respectively). Vertical scale bar, -60 mV to -50 mV. Horizontal scale bar, 1 s. (B) Simplified diagram of the pyloric circuit. The pacemaker kernel is comprised of the AB neuron and two electrically coupled PD neurons. The follower cells include a single LP neuron and several electrically coupled PY neurons. Filled circles represent inhibitory chemical synapses; resistor symbols represent electrical coupling. (C) Overlays of 3 cycles of PD, LP, and PY neuron activity recorded intracellularly at three different temperature ($T = 7^{\circ}\text{C}$, $T = 11^{\circ}\text{C}$, $T = 19^{\circ}\text{C}$; blue, black, pink, respectively) from the same preparation. These traces were scaled for cycle period and then superimposed upon one another. Vertical scale bar, 10 mV. Horizontal scale bar, 1 duty cycle. (D) Total IPSPs recorded in LP as a function of temperature from $T = 7^{\circ}\text{C}$ to $T = 23^{\circ}\text{C}$ ($n = 7$). doi:10.1371/journal.pbio.1000469.g002

outward current is observed during PY time and a much larger outward current during PD time. The waveforms seen at -80 mV are complex because the PY and AB glutamatergic IPSCs reverse at a more depolarized potential than does the cholinergic PD IPSC [15,30]. At -100 mV, all components were inward.

The synaptic currents recorded at -60 mV are most relevant to understanding the membrane potential trajectories seen during the ongoing rhythm (Figure 2A,C). Accordingly, the total IPSCs measured at -60 mV as a function of temperature are plotted in Figure 3D. These exhibit a Q_{10} of 2.29 ± 0.25 ($n = 7$). Figure 3E shows superimposed membrane potential trajectories at three temperatures, and their corresponding IPSCs recorded from the same preparation (at -60 mV). Together, these data illustrate that despite the virtually superimposable voltage trajectories, the underlying IPSCs are almost 5-fold larger at the higher temperatures. Moreover, it appears that this increase would more than compensate for the modest increase in input conductance over the same range ($Q_{10} = 1.56 \pm 0.17$; Figure 3A). This suggests that the constant waveform can only partially be accounted for by the changes in input conductance and IPSC amplitude.

Effects of Temperature on I_A and I_h

Previous work demonstrated the importance of both the transient outward current, I_A , and the hyperpolarization-activated inward current, I_h , on the phase at which the LP and PY neurons recover from inhibition [15,16,17,27]. Consequently, we measured the effects of temperature on these currents in voltage clamp,

as we hypothesized that changes in these currents could contribute to the temperature compensation of phase (Figure 1D).

Figure 4A illustrates the effects of temperature on I_A . I_A was measured as the difference current between the outward currents evoked from a holding potential of -100 mV and those evoked from -40 mV. The currents measured at voltages from -40 mV to $+30$ mV in 10 mV steps are shown at five temperatures from 7°C to 23°C (Figure 4A). As the temperature was increased, the amplitude of the peak outward current increased (Figure 4B). The activation rate as well as the inactivation rate of I_A also increased as a function of temperature (Figure 4C and 4D, respectively). The Q_{10} of the I_A inactivation rate was 3.78, the steepest temperature dependence of the parameters we measured (Table 1).

Lastly, we measured the temperature dependence of I_h . Because I_h is a depolarizing current that is activated only at hyperpolarized potentials, its properties allow I_h both to respond to inhibitory synaptic currents and to play an opposing role to I_A in determining the latency to firing after synaptic inhibition. We measured I_h using 12 second hyperpolarizing voltage steps from -50 mV to -120 mV in 5 mV steps (Figure 5A) at different temperatures. The amplitude of the current (Figure 5B) as well as its activation rate increased at higher temperatures (Table 1).

The Effects of Temperature on Models of a Bursting Pacemaker Neuron

Temperature increased the frequency of the pyloric rhythm (Figure 1). The membrane properties of the PD/AB pacemaker

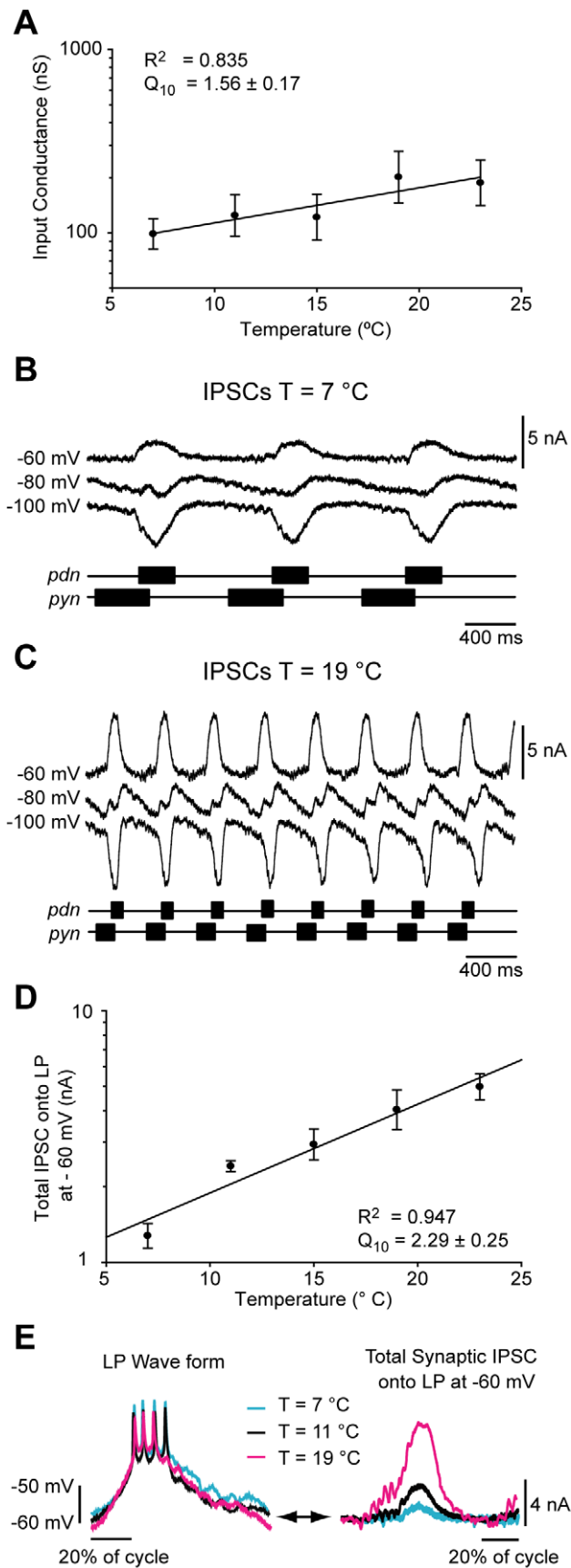


Figure 3. Input conductance and IPSCs as a function of temperature. (A) Input conductance of the LP neuron as a function of temperature was measured in the presence of 10^{-7} M TTX and 10^{-5} M PTX in the passive range (-60 to -80 mV). (B) Example IPSCs of the LP neuron recorded at cold temperature ($T=7^{\circ}\text{C}$) at holding potentials of -60 , -80 , and -100 mV. The corresponding extracellular recordings of the pyloric dilator nerve (*pdn*) and pyloric nerve (*pyn*) showing the corresponding PD and PY bursts are shown schematically. Vertical scale bar, 5 nA. Horizontal scale bar, 400 ms. (C) Example IPSCs from the same LP neuron as in (A) but at warmer temperature ($T=19^{\circ}\text{C}$). (D) Amplitude of the total IPSC at -60 mV as a function of temperature from $T=7^{\circ}\text{C}$ to $T=23^{\circ}\text{C}$ ($n=7$). (E) *Left*: Overlay of LP waveform at temperatures of 7, 19, and 23°C from the same preparation. Horizontal scale bar, 20% duty cycle. Vertical scale bar -60 to -50 mV. *Right*, overlay of the corresponding total IPSC of the LP neuron at -60 mV at temperatures of 7, 19, and 23°C . Horizontal scale bar, 20% duty cycle. Vertical scale bar, 4 nA. doi:10.1371/journal.pbio.1000469.g003

group are the most important determinant of pyloric frequency [31,32,33]. Consequently, we were interested to determine whether increases in frequency with increasing temperature in bursting neurons are to be generally expected. Therefore, we studied the effects of temperature on model bursting neurons [25], whose currents were initially based on those recorded from lobster STG neurons [34]. We first generated 1270 models, all of which were bursting at 23.5°C , but which differed in the maximal conductances of their 7 membrane currents. We then changed the temperature of all of the models, using a Q_{10} of 2 for all of the activation and inactivation rates of the currents. Figure 6 shows the effects of temperature on 7 of the 1,270 models studied and illustrates that models with differing sets of maximal conductances varied dramatically in their response to temperature.

Only 60.5% of the models showed bursting over the entire range of temperatures and increased monotonically in frequency over the full temperature range. Of this 60.5%, 68.5% maintained approximate constant duty cycle over the entire temperature range, a feature that would promote phase compensation in the network.

The remaining 39.5% of the models either did not burst over the entire range or displayed decreases in frequency over at least some of the temperature range (Figure 6B–G). Together these data indicate that the maximal conductances of the currents are important in determining how that particular neuron will behave in response to a temperature change.

The Effects of Temperature on Phase Compensation in Model LP Neurons

Taylor et al. [26] recently developed a family of 1304 LP neuron models, each of which has different values of its maximal conductances and all of which fit a set of criteria matching the biological LP neuron. We used this set of LP neuron models to ask whether the temperature dependence of I_A and I_h contribute to temperature compensation of the LP neuron's phase. Figure 7A shows the results of a simulation in which we varied the temperature of a model LP neuron. In this set of simulations, we compared two conditions: (a) all model Q_{10} 's were set to 1, and (b) the Q_{10} 's of I_A and I_h were replaced by the experimentally measured values (Figures 4 and 5). The LP onset phase typically became more delayed as the frequency was increased (Figure 7A,B,C; $p < 0.0001$, Kruskal-Wallis test, $n = 1,063$), but the biologically measured Q_{10} 's decreased this effect ($p < 0.0001$, sign test on 23°C data, $n = 1,063$) and increased the extent to which the LP maintained constant phase as a function of temperature.

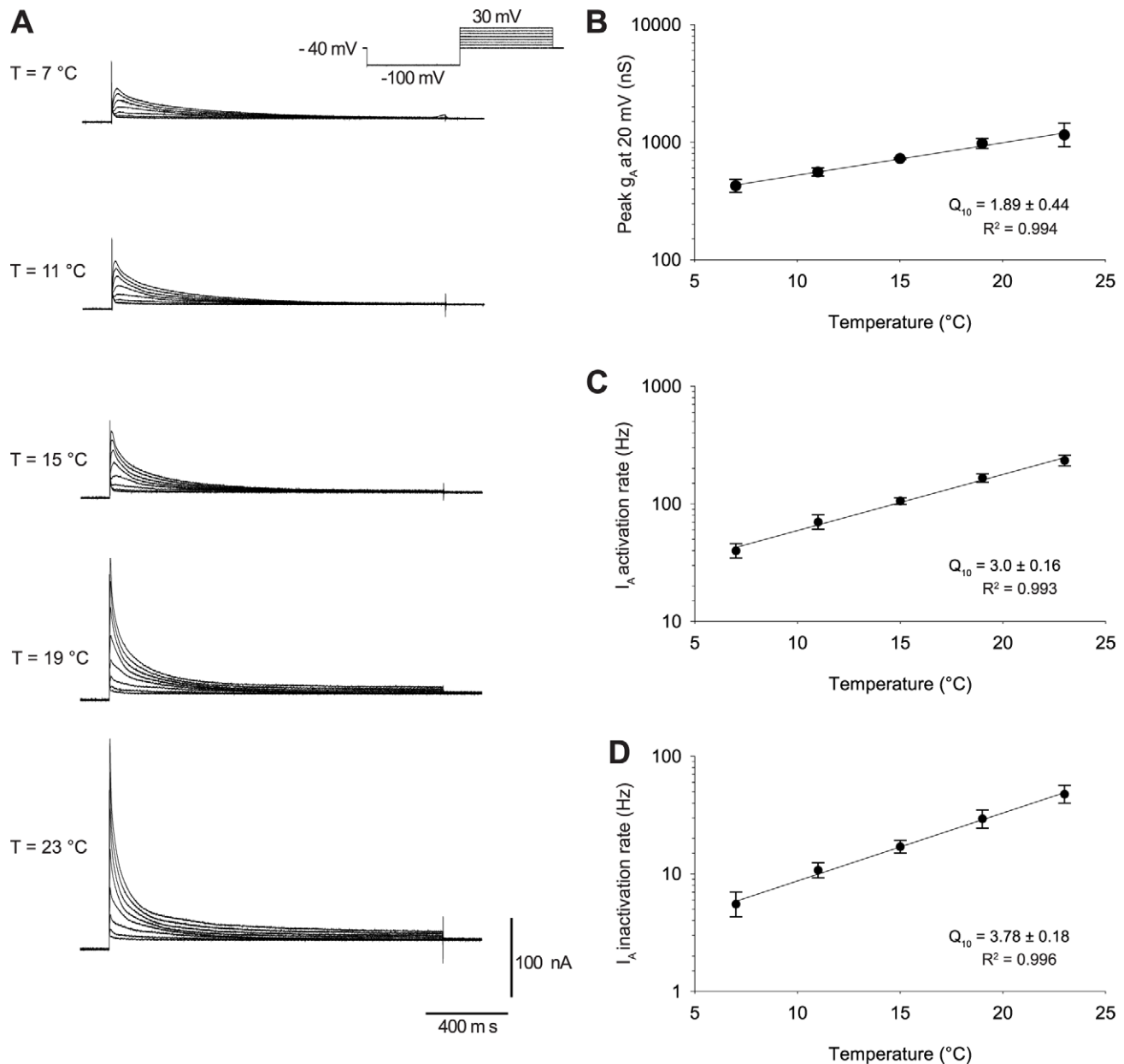


Figure 4. Temperature dependence of I_A conductance, activation rate, and inactivation rate. (A) Family of I_A currents at 7, 11, 15, 19, and 23°C elicited in response to depolarizing steps from -40 mV to +30 mV in 10 mV steps. (B) Pooled data for the temperature dependence of I_A peak conductance measured at +20 mV ($n=6$). (C) Temperature dependence of I_A activation rates was measured as the reciprocal of the time to maximal current elicited at +20 mV (from the time of the depolarizing step). (D) Temperature dependence of I_A inactivation rates was measured as the reciprocal of the time to decay to half of the maximal current from the time of maximal current elicited at +20 mV. doi:10.1371/journal.pbio.1000469.g004

We then examined the effects of changing all of the model Q_{10} 's to 1.5, 2.0, and 3.0 (Figure 7D,E,F, respectively) and again compared the effects of using these default Q_{10} 's for I_A and I_h (blue) to the condition in which they had the experimentally determined values (red). These plots show that in the "default" (blue) condition, temperature affected the LP onset phase for all Q_{10} 's ($p < 0.0001$ for all three Q_{10} 's, Kruskal-Wallis test, $n = 1,148, 1,255,$ and $1,109,$ respectively). For the blue condition, LP onset phase came later at high temperatures for $Q_{10} = 1.5$, became approximately temperature compensated for $Q_{10} = 2.0$, and became considerably "overcompensated" for $Q_{10} = 3.0$ (slopes were significantly different, $p < 0.0001$, Kruskal-Wallis test, $n = 1,012$). Note that the differences between the red and blue

conditions were smaller for larger Q_{10} values (at 23°C, there was a significant effect of Q_{10} on the difference between red and blue conditions, $p < 0.0001$, Kruskal-Wallis test, $n = 1,138$; all pairwise differences between Q_{10} 's were significant at $p < 0.0001$, rank sum test with Bonferroni correction).

Discussion

Poikilotherms often face considerable temperature fluctuations during a given day or over extended periods of time. This poses a series of interesting questions for the nervous system, as it needs to maintain its important functions despite these environmental perturbations. Many previous studies have documented the effects

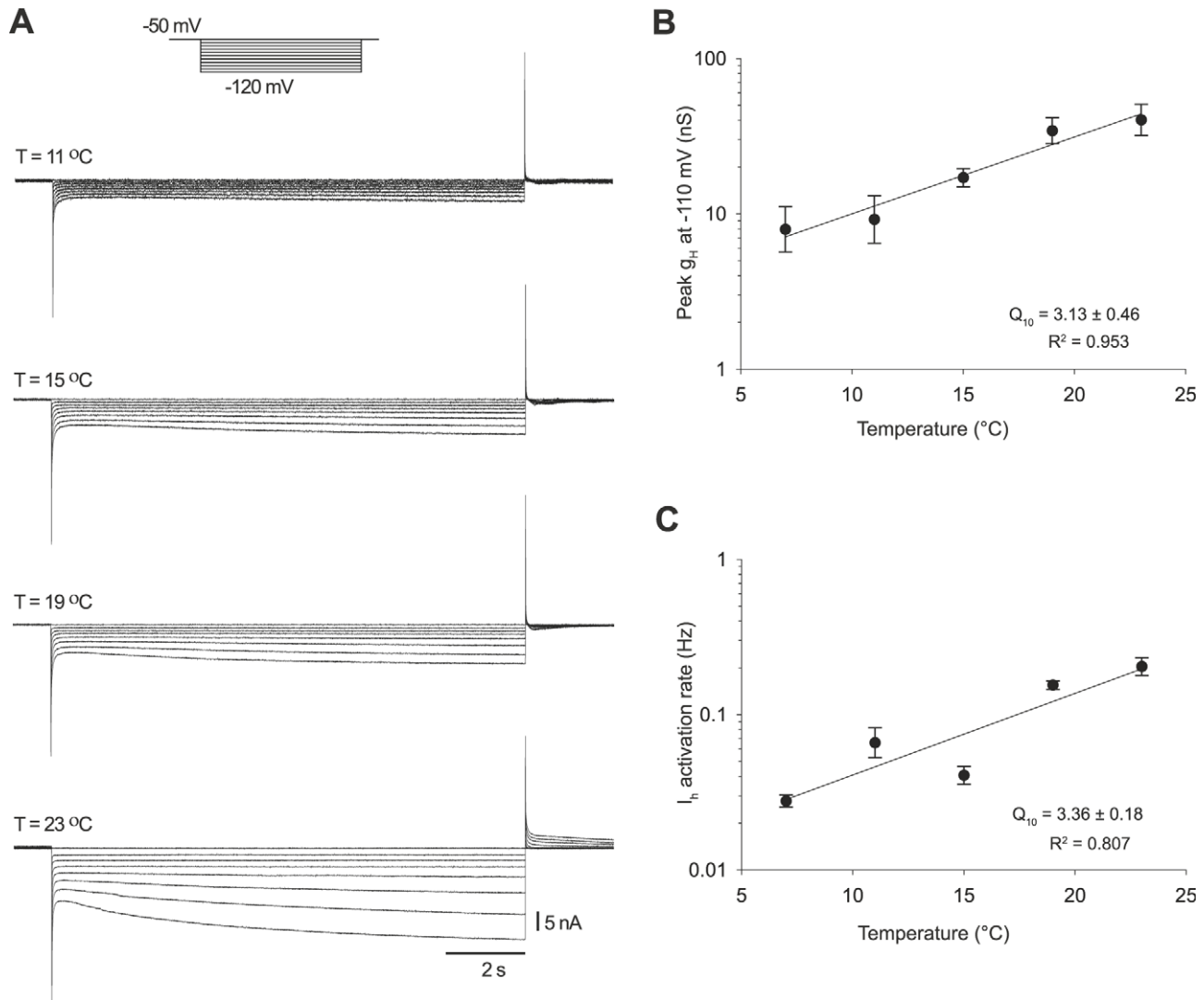


Figure 5. Temperature dependence of I_h conductance and activation rate. (A) Family of I_h currents at 11, 15, 19, and 23°C elicited in response to hyperpolarizing steps from -50 mV to -120 mV in 5 mV steps from a holding potential of -50 mV (10 mV steps shown here). (B) Pooled data for the temperature dependence of I_h peak conductance measured at -110 mV ($n=7$). (C) Temperature dependence of I_h activation rates were measured as the reciprocal of the activation time constants obtained from single exponential fits of the current at -110 mV ($n=7$). doi:10.1371/journal.pbio.1000469.g005

of temperature on a variety of behaviors and physiological processes [3,35,36,37,38,39]. Other studies have looked at the effects of temperature on individual biochemical reactions, ion channels, synapses, or other cellular mechanisms [6,40,41,42, 43,44,45]. Nonetheless, much less work has been done directly on the effects of temperature on behaviorally relevant neuronal circuits. This study is one of relatively few to attempt to account for the effects of temperature on a neuronal circuit in terms of the cellular processes that contribute to those circuit behaviors.

The General Problem of Temperature Compensation

By convention, processes with Q_{10} 's less than 2 are considered to be relatively temperature insensitive, and behaviors with emergent system Q_{10} 's less than 2 are conventionally termed "temperature compensated." The best known example of temperature compensation is that shown by the circadian rhythm, and its temperature compensation is considered one of its salient features. Although the molecular basis underlying circadian rhythms have been well-elucidated [1], the mechanisms that

underlie their temperature compensation remain unresolved. However, a recent study on temperature compensation in *Neurospora* [2] argues that temperature compensation arises from compensatory changes in the rates of phosphorylation and degradation of proteins that are part of the molecular clock.

Zhurov and Brezina [46] have provided an elegant study of a different form of temperature compensation in the *Aplysia* neuromuscular system. In this preparation, the strength of neuromodulatory effects on muscle contraction was maintained over a temperature range from 15°C to 25°C. Paradoxically, the release of neuromodulators that modulate neuromuscular contraction decreased 20-fold when temperature was increased. However, the decrease in neuromodulator release was partially compensated by increased neuromodulator efficacy. Thus in this particular example, physiological temperature compensation is achieved by opposing temperature dependencies of related functions.

In this study, we describe a form of temperature compensation that occurs in a rhythmically active neural circuit. When we rapidly varied the temperature of the in vitro stomatogastric

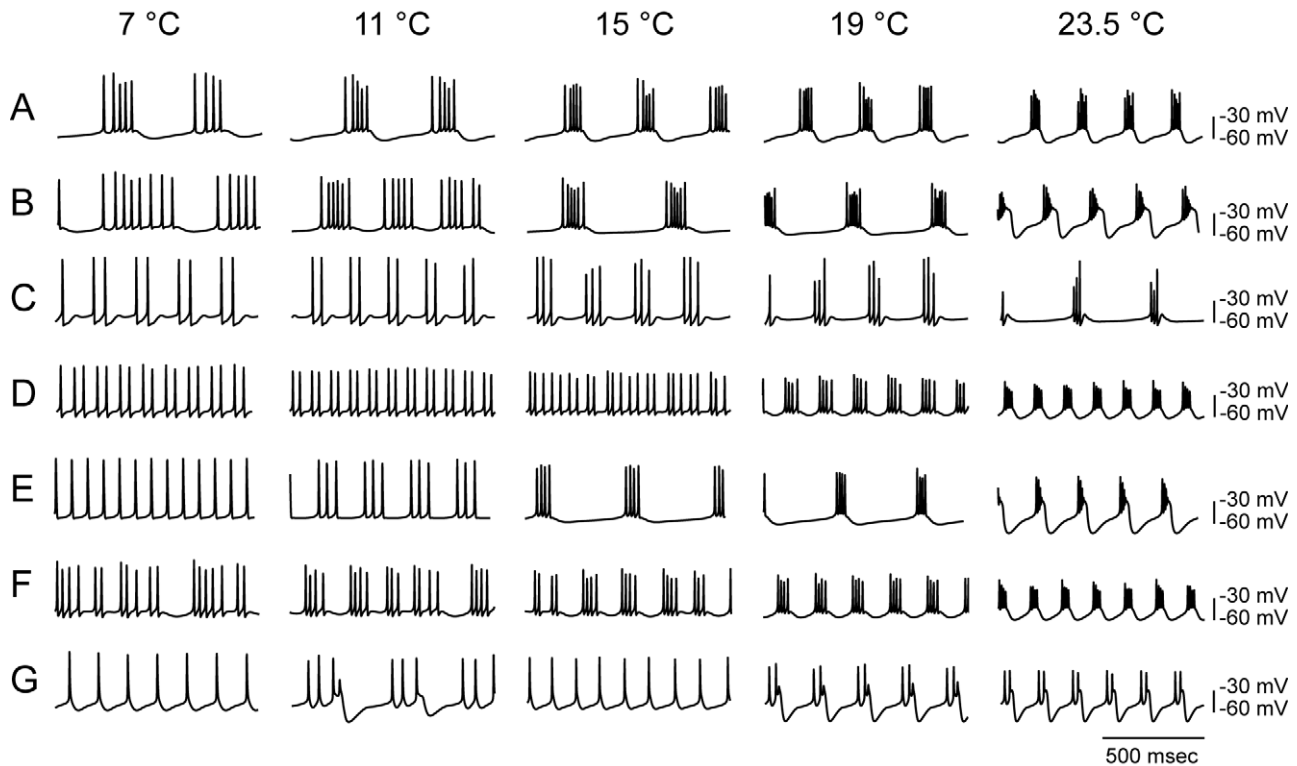


Figure 6. Diverse electrical behavior of model bursting neurons in response to changing temperature. Examples that illustrate the diversity of firing patterns of simulated model neurons in response to changing temperatures from 23.5°C to 7°C. (A) Neuron that increases burst frequency as a function of temperature. (B) Neuron that decreases burst frequency sharply from 11 to 15°C, then subsequently increases with temperature. (C) Neuron that decreases burst frequency from 11 to 23.5°C. (D) Neuron that transitions from tonic spiking to bursting behavior at 19°C. (E) Neuron that transitions from tonic spiking at 11°C, then increases burst frequency with increase in temperature. (F) Neuron that transitions from irregular spiking to bursting behavior. (G) Neuron that switches its firing pattern twice: the neuron tonically spikes at 7°C, bursts at 11°C, reverts to spiking at 15°C, and then switches to bursting at 19 and 23.5°C.
doi:10.1371/journal.pbio.1000469.g006

nervous system, the pyloric network frequency varied about 4-fold, from ~ 0.7 Hz at low temperatures to ~ 2.9 Hz at 23°C (Figure 1C). At the same time, the phase relationships of the pyloric rhythm were tightly maintained over this large frequency range (Figure 1). The almost perfect temperature compensation of pyloric rhythm phase (Table 1) described here surpasses that described in many systems, including some circadian rhythms [2,46].

All of the component processes we measured increased in amplitude and/or rate with temperature. However, given that some of these component processes—e.g., I_A and I_h —have opposing functional roles, temperature compensation of the phase relationships of the pyloric neurons appears to emerge as a consequence of similar temperature dependencies of opposing cellular mechanisms. Figure 8 shows a cartoon of the main processes that are likely to control the phase of the LP neuron's activity. LP's activity is terminated by PY neuron activity, and then additionally inhibited by the AB/PD neurons during the pacemaker burst. Rebound firing after the AB/PD burst is enhanced by I_h activation and delayed by I_A activation [17,27]. An increase in the IPSC amplitude will tend to increase the activation of I_h and also favor the voltage-dependent deinactivation of I_A . Consequently, as temperature increases, these opposing time and voltage-dependent processes, as a first approximation, may remain temporally scaled with each other. The LP off-phase is determined by the phase of PY onset, which is itself maintained constant, presumably by similar mechanisms.

Phase and Frequency in Motor Systems

At constant temperature, the pyloric network phase relationships are also maintained despite changes in frequency [13,15,19,21,22,23,47]. This has been extensively studied because it is not obvious how to turn the constant delays associated with the fixed dynamics of synaptic currents or other membrane currents into a mechanism that confers phase constancy. Again, as illustrated in Figure 8, it has been suggested that the latency to firing of a follower neuron is controlled by multiple processes, including synaptic depression, I_A , and I_h [20,48]. At constant temperature, the frequency dependence of synaptic depression of the AB/PD IPSP is balanced by the time-dependence of activation of I_h and deinactivation of I_A [24].

Thus, the mechanisms that allow for phase maintenance at constant temperature seem to employ some of the same cellular mechanisms that promote temperature compensation. This is not necessarily surprising, because the strong evolutionary pressure that gave rise to robust phase maintenance may have also forced a set of solutions that would be robust enough to compensate for the frequency changes that arise from changes in temperature.

The ability to maintain phase independent of frequency has been well-described in the neuronal control of swimming in lamprey, leech, and crayfish [49,50,51]. In these systems, phase is constant over a wide range of frequencies [49,50,51], and it would be interesting to see how well temperature compensated they are. It is surprising that in the zebra finch, a homeotherm, in which singing behavior is highly stereotyped, cooling specific brain areas

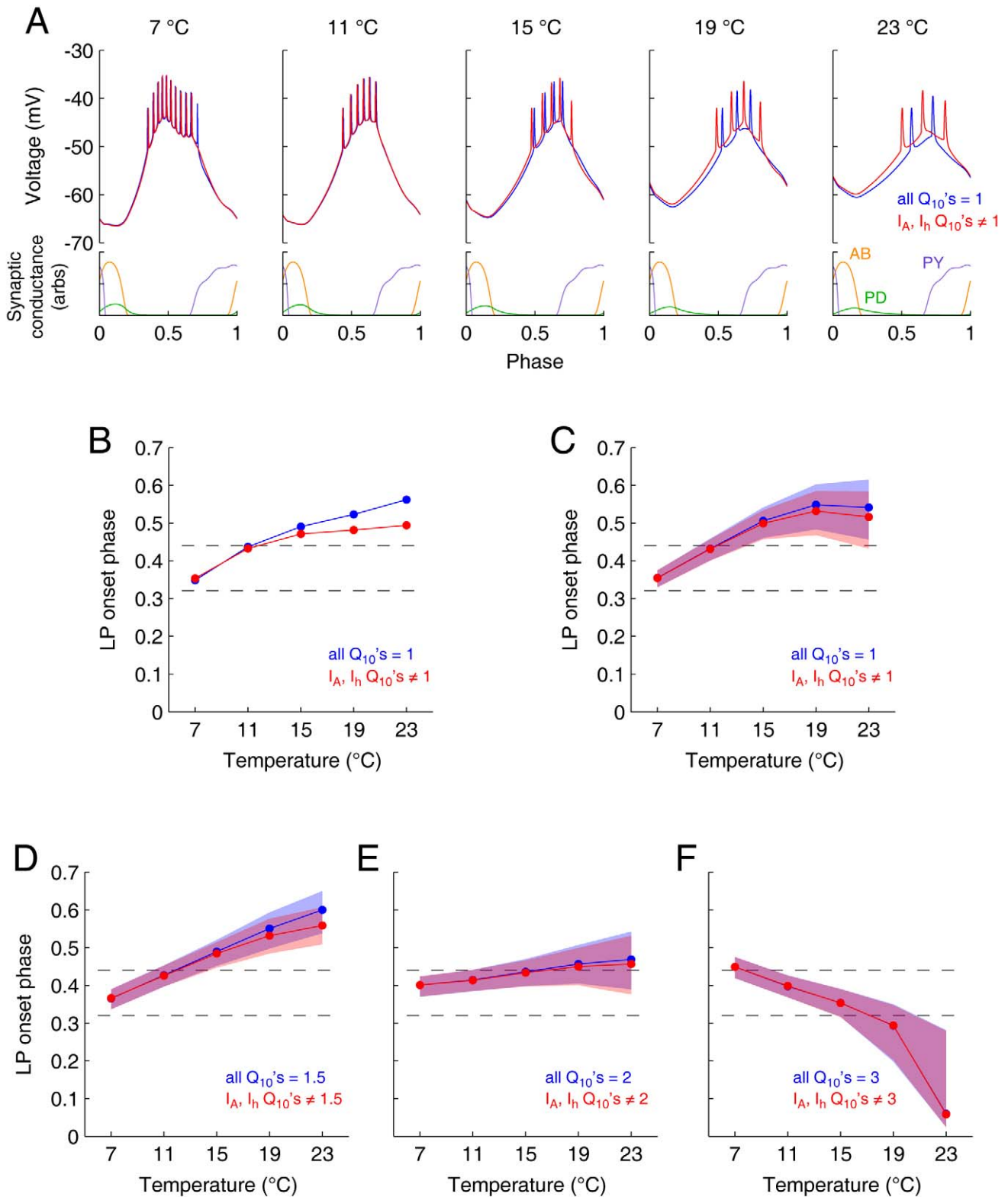


Figure 7. Effects of temperature on a population of 1304 LP models. (A) Voltage traces of an example LP model at different temperatures, for a single cycle of simulated pyloric synaptic input. Blue traces are for a model with all Q_{10} 's set to one. Red traces are the same model, but with the Q_{10} 's for I_A and I_h set to their measured values. Lower panels show the synaptic conductances injected into the model. At each temperature, the synaptic input had a frequency as given by the linear fit in Figure 1C. The x-axis in each panel has been scaled to show the voltage versus phase. (B) LP onset phase versus temperature for the same model as shown in (A). Dashed lines here and in other panels show the bounds of the central ~85% of the distribution of LP phase onsets observed experimentally [15]. (C) LP onset phase versus temperature for all 1,304 models. Line shows the median LP onset phase for all models that fired at that temperature. Shaded region shows the range of the 25th to 75th percentile. (D) Blue

simulations had a Q_{10} of 1.5 for all intrinsic conductances, and the red simulations had the Q_{10} 's for I_A and I_h set to their measured values. (E) A "default" Q_{10} of 2.0 for all intrinsic conductances. (F) Default Q_{10} of 3.0. Note that (A), (B), and (C) are not directly comparable with (D), (E), and (F), because (A), (B), and (C) had a Q_{10} of 1.0 for the synaptic conductances, whereas (D), (E), and (F) used the experimentally measured Q_{10} of 2.3 for the synaptic conductances.

doi:10.1371/journal.pbio.1000469.g007

in the motor pathway leads to uniform elongation of the song [52]. We speculate that the strong temperature dependence of frequency and temperature-independence of phase may not be unique to the pyloric circuit of the stomatogastric nervous system and may be a useful property to other animals, allowing them to cope with environmental challenges in their natural setting.

The Effects of Temperature on Frequency and Phase in Computational Models

Our commonsense knowledge of the world may lead us to believe that achieving robust behavior in cold-blooded animals over a range of temperature is simpler than it is in fact. The non-trivial nature of this problem is revealed in the computational studies reported here. In both cases, we employed families of more than 1,000 model neurons that varied in terms of the maximal conductances of their underlying currents but were otherwise identical. These modeling studies illustrate the extent to which robust physiological behavior requires that the temperature dependence of the biological processes must be closely regulated.

Many of the 1,270 pacemaker models (Figure 6) failed to maintain a bursting phenotype over the entire temperature range or else showed interesting non-monotonic changes in frequency. In some cases bursting frequency decreased as temperature increased between certain temperature points (Figure 6B and E) or along the entire temperature range (Figure 6C). One implication of this model is that not all combinations of currents that give rise to bursting at one temperature will necessarily provide robust behavior at other temperatures. Furthermore, the requirement that a neuron or group of neurons show increased burst frequency in a clean monotonic fashion as temperature is increased may

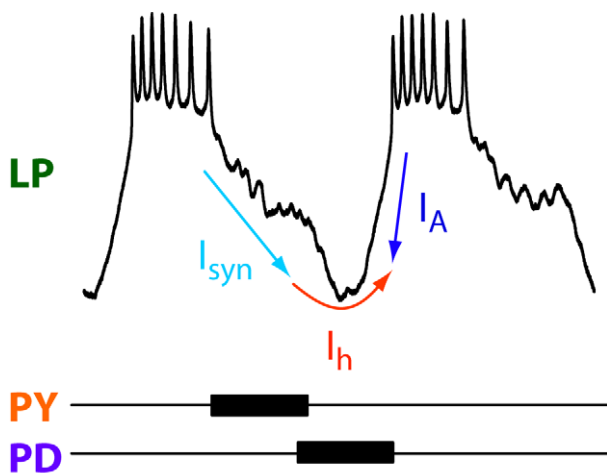


Figure 8. Schematic of the processes that contribute to the control of phase in the LP neuron. LP neuron activity is terminated by inhibitory synaptic input (light blue arrow) and the onset of this synaptic input is initiated by the PY neurons (orange). PY neuron activity continues until the PD/AB neurons start to fire (purple), at which time the PD/AB neurons strongly inhibit the LP neuron. After the end of the PD/AB burst, the LP starts firing with a delay that is decreased by activation of I_h (red arrow) and increased by the activation of I_A (dark blue arrow).

doi:10.1371/journal.pbio.1000469.g008

considerably restrict the parameter space in which "good enough" solutions may reside.

Although there has been a good deal of both experimental and theoretical work on the importance of both I_A and I_h in determining phase in the pyloric network, without the computational studies shown in Figure 7, it was difficult to know whether the specific Q_{10} 's of I_A and I_h would favor temperature compensation of phase. The first result from these studies (Figure 7C) was that the measured Q_{10} 's of I_A and I_h promote temperature compensation of phase. This effect was most pronounced when it was examined with a background of low Q_{10} 's of the other currents in the models (Figure 7C,D). When the background Q_{10} 's were higher (Figure 7E,F), although I_A and I_h still statistically altered the phase onset of the LP neuron, the extent of their influence decreased.

Taken at face value, the data we obtained with the 1,304 LP neuron models (Figure 7) suggest that temperature compensation of phase will be optimized when the Q_{10} 's of all of the currents that contribute to phase are close to the Q_{10} of the pyloric rhythm frequency, which was ~ 2.3 (Figure 1).

General Implications

Although it is possible for the same neuron in different animals to have widely disparate sets of current densities for ion channels [15,53,54], the Q_{10} 's of these currents and other biological processes must be presumably regulated within a certain range. The actual number of enzyme molecules or ion channels in a given neuron in an individual animal may vary widely according to the life history of the animal. On the other hand, the temperature-dependence of biological enzymes and ion channels has arisen as a result of evolution working on the structure of each protein molecule, so one would naively predict that the Q_{10} 's of a given process measured across animals of the same species might vary less than the number of ion channels or enzyme molecules. Of course, post-translational and other history-dependent processes could also influence the Q_{10} 's of many biological processes, so the process of producing both robust behavior and temperature compensation over a large temperature range requires the coordinated regulation of myriad biological processes.

Methods

Animals

Cancer borealis were purchased from Commercial Lobster (Boston, MA) and maintained in tanks containing artificial seawater at 11°C for 3 wk before use.

Solutions

C. borealis physiological saline was composed of 440 mM NaCl, 11 mM KCl, 13 mM CaCl₂, 26 mM MgCl₂, 11 mM Trizma base, and 5 mM Maleic acid, pH 7.4–7.5. All reagents were purchased from Sigma Aldrich.

Electrophysiology

The stomatogastric nervous system was dissected out of the animals and pinned out in a Sylgard (Dow Corning) coated plastic Petri dish containing chilled saline (11°C). In all cases, we worked only with fully intact stomatogastric nervous system preparations

that included the commissural and esophageal ganglia with two intact superior esophageal nerves and two intact inferior esophageal nerves.

The preparations were continuously superfused with physiological saline. The temperature of the superfusing saline was controlled using a Peltier device purchased from Warner Instruments. The temperature was changed at about 1 degree/min when only extracellular recordings were made and about 1 degree/2–3 min when intracellular recordings were also made. As the temperature was increased we noticed that the ganglia swelled and/or moved. This often necessitated small movements of the intracellular electrodes (up or down, respectively, as the temperature was increased or decreased) to maintain the intracellular recordings. When the electrodes were repositioned carefully, return to 11°C showed no changes in resting potential, firing properties, or input resistance. If the electrodes were not repositioned slightly, penetrations were usually lost with large temperature changes. The preparations were maintained at their target temperature for 10 min before data were taken.

Vaseline wells were placed around motor nerves and extracellular recordings were obtained using stainless steel pin electrodes placed in the wells and amplified using an A-M Systems differential amplifier. Intracellular recordings were obtained from cell bodies in the STG using 10–30 M Ω glass microelectrodes pulled with a Flaming/Brown micropipette puller (Sutter Instrument, Co.) The microelectrode solution contained 0.6 M K₂SO₄ and 20 mM KCl. Data were acquired using a Digidata 1200 data acquisition board (Axon Instruments) and analyzed using Clampfit 9.0 (Axon Instruments) Spike2 v 6.04 (Cambridge Electronic Design) and/or MATLAB 7.1 (Mathworks). Statistical analyses were performed using the SigmaPlot 10 and SigmaStat software packages (Jandel Scientific).

Input conductance was measured in two electrode voltage clamp by stepping the membrane from –60 mV to –80 mV in 5 mV steps, measuring the resulting currents, and then calculating the conductance.

IPSCs were measured using two electrode voltage clamp during the ongoing rhythm. IPSCs were measured in the LP neuron at membrane potentials from –60 mV to –120 mV in 5 mV steps. Each holding potential was maintained for 8–12 s, and the membrane potential was returned to –60 mV in between each voltage step for at least 8–12 s.

I_h and I_A were both measured in the presence of 10^{–7} M TTX, 10^{–5} M PTX, and 10^{–2} M TEA. I_h was measured at membrane potentials from –50 mV to –120 mV in 5 mV steps using 12 s pulses with 12 s at –50 mV between each pulse. I_A was measured as the difference current between steps taken from a holding potential of –100 mV and those taken from a holding potential of –40 mV. Currents were recorded from –40 mV to +30 mV at 10 mV intervals using pulses of 1.5 s following a 1.5 s prepulse.

Q₁₀ Calculations

To characterize and compare the temperature dependencies of various parameters of the pyloric network, we used a modified Arrhenius equation to determine the temperature coefficient, Q₁₀. The Q₁₀ is a conventional measure used to describe how much a given rate process changes over a 10°C temperature change and defined as [rate(T+10°)/rate(T)] [55]. A given parameter *p* was plotted against temperature T in a semilog plot and the Q₁₀ value was then extracted from the slope of the linear regression (*m*) [3].

$$Q_{10} = 10^{10m} \quad (1)$$

$$m = \frac{d \log P}{dT} \quad (2)$$

The standard error of the Q₁₀ (*se*_{Q₁₀}) was calculated by propagation error from the slope and the standard error of the slope (*se*_{*m*}) of the linear regression [56]:

$$se_{Q_{10}} = se_m \cdot \ln 10 \cdot 10^{10m+1} \quad (3)$$

Although the alternative Arrhenius activation energy values are implicit in our analyzed data, we did not express this more physical description due to the non-unitary nature of our parameters (i.e., they are not simple processes with a single rate-limiting barrier).

The Bursting Pacemaker Models

The model used to simulate bursting neurons has been previously described [25]. Briefly, this contains seven active voltage-dependent conductances, a leak conductance, and an algorithm for activity-dependent homeostatic regulation of maximal channel conductances. We added to this model the ability to control the temperature sensitivity (Q₁₀) of all channel activation and inactivation dynamics. For simplicity we set the Q₁₀ of all the activation and inactivation rates equal to 2. All values for *m_∞*, *h_∞*, *τ_m*, *τ_h*, and *p* are as found in Liu et al. [25] but modified to incorporate the Q₁₀.

To create a population of model bursting neurons, we initiated 1,500 simulations with random initial values for all seven active conductances. Each model was subject to 1 h of simulated activity-dependent homeostatic regulation at the model's default temperature of 23.5°C. Models that showed poor bursting behavior after this period were excluded, resulting in a population of 1,270 model neurons that were bursting at 23.5°C and which had a variety of different values of the maximal conductances for the voltage-dependent currents. We then turned off the self-tuning function in these neurons and used them as a set of models with different underlying conductances to probe the extent to which they maintained functional bursting activity over a wide range of temperatures.

Each model was run at 7, 11, 15, and 19°C—the same temperatures used in the biological studies. Voltage traces from each of these simulations were analyzed to determine how the bursting behavior varied with temperature. Bursting behavior—as measured by slow wave frequency—was extracted from each simulation using auto-correlation of a 10 s sample of the voltage trace. Here we define slow wave frequency as low-frequency membrane oscillations. We identified the frequency of these oscillations as the lowest frequency peak in the autocorrelogram of the voltage waveform. If this peak had an autocorrelation less than 0.05, we instead used the frequency corresponding to the greatest autocorrelation (this is uncommon and corresponds to very irregular activity).

To determine whether the bursting neurons maintained duty cycle as a function of temperature, we calculated the coefficient of variation (CV) of each model's duty cycle. The bounds used to define the population of model bursting neurons that exhibited “constant duty cycle” were chosen to contain the central ~85% of the experimental data (PD off phase). Models exhibiting CVs of duty cycle across temperature within this bound were classified as having constant duty cycle, while those with CVs above this value were classified as having a “non-constant duty cycle.”

The LP Neuron Models

Simulations to determine how the Q_{10} 's of I_A and I_h affect LP phase onset were performed using the LP model described in Taylor et al. [26]. This model was modified so that Q_{10} 's could be associated with all voltage-gated and synaptic conductances. For each voltage-gated conductance, there was a Q_{10} for the maximal conductance, another for the activation rate, and another for the inactivation rate. The reference temperature was 10°C, as the model was originally designed to mimic LP's behavior at this

temperature. Reversal potentials (and the GHK relation for the calcium current) were not changed with temperature, as these effects are small over the temperature range used.

Author Contributions

The author(s) have made the following declarations about their contributions: Conceived and designed the experiments: LST ALT EM. Performed the experiments: LST MLG JSC ALT MF. Analyzed the data: LST MLG JSC ALT MF. Wrote the paper: LST EM.

References

- Rosbash M (2009) The implications of multiple circadian clock origins. *PLoS Biol* 7: e62. doi:10.1371/journal.pbio.100062.
- Mehra A, Shi M, Baker CL, Colot HV, Loros JJ, et al. (2009) A role for casein kinase 2 in the mechanism underlying circadian temperature compensation. *Cell* 137: 749–760.
- Lenz PH, Hower AE, Hartline DK (2005) Temperature compensation in the escape response of a marine copepod, *Calanus finmarchicus* (Crustacea). *Biol Bull* 209: 75–85.
- Cao XJ, Oertel D (2005) Temperature affects voltage-sensitive conductances differentially in octopus cells of the mammalian cochlear nucleus. *J Neurophysiol* 94: 821–832.
- Moran MM, Xu H, Clapham DE (2004) TRP ion channels in the nervous system. *Curr Opin Neurobiol* 14: 362–369.
- Peloquin JB, Doering CJ, Rehak R, McRory JE (2008) Temperature dependence of Cav1.4 calcium channel gating. *Neuroscience* 151: 1066–1083.
- DFO (2009) *Can Sci Adv Sci Sec Adv Rep* 034.
- Stehlik LL, MacKenzie CL, Morse WW (1991) Distribution and abundance of four brachyuran crabs on the northwest Atlantic shelf. *Fish Bull*, U S 89: 473–492.
- Haeflner PA (1977) Aspects of the biology of the Jonah crab, *Cancer borealis* Stimpson, 1859 in the mid Atlantic Bight. *J Nat Hist* 11: 303–320.
- Donahue MJ, Nichols A, Santamaria CA, League-Pike PE, Krediet CJ, et al. (2009) Predation risk, prey abundance, and the vertical distribution of three brachyuran crabs on Gulf of Maine shores. *Journal of Crustacean Biology* 29: 523–531.
- Krediet CJ, Donahue MJ (2009) Growth-mortality trade-offs along a depth gradient in *Cancer borealis*. *Journal of Experimental Marine Biology and Ecology* 373: 133–139.
- Maynard DM, Dando MR (1974) The structure of the stomatogastric neuromuscular system in *Callinectes sapidus*, *Homarus americanus* and *Panulirus argus* (decapoda crustacea). *Philos Trans R Soc Lond (Biol)* 268: 161–220.
- Eisen JS, Marder E (1984) A mechanism for production of phase shifts in a pattern generator. *J Neurophysiol* 51: 1375–1393.
- Hartline DK, Gassie DV, Jr. (1979) Pattern generation in the lobster (*Panulirus*) stomatogastric ganglion. I. Pyloric neuron kinetics and synaptic interactions. *Biol Cybern* 33: 209–222.
- Goaillard JM, Taylor AL, Schulz DJ, Marder E (2009) Functional consequences of animal-to-animal variation in circuit parameters. *Nat Neurosci* 12: 1424–1430.
- Harris-Warrick RM, Coniglio LM, Barazangi N, Guckenheimer J, Gueron S (1995) Dopamine modulation of transient potassium current evokes phase shifts in a central pattern generator network. *J Neurosci* 15: 342–358.
- Tierney AJ, Harris-Warrick RM (1992) Physiological role of the transient potassium current in the pyloric circuit of the lobster stomatogastric ganglion. *J Neurophysiol* 67: 599–609.
- Rabbah P, Nadim F (2005) Synaptic dynamics do not determine proper phase of activity in a central pattern generator. *J Neurosci* 25: 11269–11278.
- Bucher D, Prinz AA, Marder E (2005) Animal-to-animal variability in motor pattern production in adults and during growth. *J Neurosci* 25: 1611–1619.
- Greenberg I, Manor Y (2005) Synaptic depression in conjunction with A-current channels promote phase constancy in a rhythmic network. *J Neurophysiol* 93: 656–677.
- Manor Y, Bose A, Booth V, Nadim F (2003) Contribution of synaptic depression to phase maintenance in a model rhythmic network. *J Neurophysiol* 90: 3513–3528.
- Hooper SL (1997) Phase maintenance in the pyloric pattern of the lobster (*Panulirus interruptus*) stomatogastric ganglion. *J Comput Neurosci* 4: 191–205.
- Hooper SL (1997) The pyloric pattern of the lobster (*Panulirus interruptus*) stomatogastric ganglion comprises two phase maintaining subsets. *J Comput Neurosci* 4: 207–219.
- Mouser C, Nadim F, Bose A (2008) Maintaining phase of the crustacean triphasic pyloric rhythm. *J Math Biol* 57: 161–181.
- Liu Z, Golowasch J, Marder E, Abbott LF (1998) A model neuron with activity-dependent conductances regulated by multiple calcium sensors. *J Neurosci* 18: 2309–2320.
- Taylor AL, Goaillard JM, Marder E (2009) How multiple conductances determine electrophysiological properties in a multicompartment model. *J Neurosci* 29: 5573–5586.
- Harris-Warrick RM, Coniglio LM, Levini RM, Gueron S, Guckenheimer J (1995) Dopamine modulation of two subthreshold currents produces phase shifts in activity of an identified motoneuron. *J Neurophysiol* 74: 1404–1420.
- Hartline DK (1979) Pattern generation in the lobster (*Panulirus*) stomatogastric ganglion. II. Pyloric network simulation. *Biol Cybern* 33: 223–236.
- Rabbah P, Nadim F (2007) Distinct synaptic dynamics of heterogeneous pacemaker neurons in an oscillatory network. *J Neurophysiol* 97: 2239–2253.
- Eisen JS, Marder E (1982) Mechanisms underlying pattern generation in lobster stomatogastric ganglion as determined by selective inactivation of identified neurons. III. Synaptic connections of electrically coupled pyloric neurons. *J Neurophysiol* 48: 1392–1415.
- Ayali A, Harris-Warrick RM (1999) Monoamine control of the pacemaker kernel and cycle frequency in the lobster pyloric network. *J Neurosci* 19: 6712–6722.
- Hooper SL, Marder E (1987) Modulation of the lobster pyloric rhythm by the peptide proctolin. *J Neurosci* 7: 2097–2112.
- Soto-Trevino C, Rabbah P, Marder E, Nadim F (2005) Computational model of electrically coupled, intrinsically distinct pacemaker neurons. *J Neurophysiol* 94: 590–604.
- Turrigiano GG, LeMasson G, Marder E (1995) Selective regulation of current densities underlies spontaneous changes in the activity of cultured neurons. *J Neurosci* 15: 3640–3652.
- Szabo TM, Brookings T, Preuss T, Faber DS (2008) Effects of temperature acclimation on a central neural circuit and its behavioral output. *J Neurophysiol* 100: 2997–3008.
- Garlick KM, Robertson RM (2007) Cytoskeletal stability and heat shock-mediated thermoprotection of central pattern generation in *Locusta migratoria*. *Comp Biochem Physiol A Mol Integr Physiol* 147: 344–348.
- Shoemaker KL, Robertson RM (1998) Flight motor patterns of locusts responding to thermal stimuli. *Journal of Comparative Physiology A-Sensory Neural and Behavioral Physiology* 183: 477–488.
- Cossins AR, Bowler K (1987) *Temperature biology of animals*. London: Chapman and Hall. 339 p.
- Neumeister H, Ripley B, Preuss T, Gilly WF (2000) Effects of temperature on escape jetting in the squid *Loligo opalescens*. *J Exp Biol* 203: 547–557.
- Nouvian R (2007) Temperature enhances exocytosis efficiency at the mouse inner hair cell ribbon synapse. *J Physiol* 584: 535–542.
- Klyachko VA, Stevens CF (2006) Temperature-dependent shift of balance among the components of short-term plasticity in hippocampal synapses. *J Neurosci* 26: 6945–6957.
- Robertson RM (1993) Effects of temperature on synaptic potentials in the locust flight system. *J Neurophysiol* 70: 2197–2204.
- Heitler WJ, Edwards DH (1998) Effect of temperature on a voltage-sensitive electrical synapse in crayfish. *J Exp Biol* 201: 503–513.
- Johnson BR, Peck JH, Harris-Warrick RM (1991) Temperature sensitivity of graded synaptic transmission in the lobster stomatogastric ganglion. *J Exp Biol* 156: 267–285.
- Johnson BR, Peck JH, Harris-Warrick RM (1992) Elevated temperature alters the ionic dependence of amine-induced pacemaker activity in a conditional burster neuron. *J Comp Physiol [A]* 170: 201–209.
- Zhurov Y, Brezina V (2005) Temperature compensation of neuromuscular modulation in *Aphysia*. *J Neurophysiol* 94: 3259–3277.
- Nadim F, Manor Y (2000) The role of short-term synaptic dynamics in motor control. *Curr Opin Neurobiol* 10: 683–690.
- Bose A, Manor Y, Nadim F (2004) The activity phase of postsynaptic neurons in a simplified rhythmic network. *J Comput Neurosci* 17: 245–261.
- Wallén P, Williams TL (1984) Fictive locomotion in the lamprey spinal cord in vitro compared with swimming in the intact and spinal animal. *J Physiol* 347: 225–239.
- Kristan WBJ, Stent GS, Ort CA (1974) Neuronal control of swimming in the medicinal leech. III. Impulse patterns of the motor neurons. *J Comp Physiol* 94: 155–176.
- Braun G, Mulloney B (1993) Cholinergic modulation of the swimmeret motor system in crayfish. *J Neurophysiol* 70: 2391–2398.
- Long MA, Fee MS (2008) Using temperature to analyse temporal dynamics in the songbird motor pathway. *Nature* 456: 189–194.
- Schulz DJ, Goaillard JM, Marder E (2006) Variable channel expression in identified single and electrically coupled neurons in different animals. *Nat Neurosci* 9: 356–362.

54. Schulz DJ, Goillard JM, Marder EE (2007) Quantitative expression profiling of identified neurons reveals cell-specific constraints on highly variable levels of gene expression. *Proc Natl Acad Sci U S A* 104: 13187–13191.
55. Hille B (2001) *Ion channels of excitable membranes*. Sunderland, MA: Sinauer. 814 p.
56. Taylor J (1997) *An introduction to error analysis: the study of uncertainties in physical measurements*. Sausalito CA: University Science Books. 323 p.